

## Linear and nonlinear optical properties of a series of Ni-dithiolene derivatives

Luis Serrano-Andrés,<sup>1,a)</sup> Aggelos Avramopoulos,<sup>2,3,a)</sup> Jiabo Li,<sup>4</sup> Pierre Labéguerie,<sup>2,5</sup> Didier Bégué,<sup>5</sup> Vladimir Kellö,<sup>6</sup> and Manthos G. Papadopoulos<sup>2,a)</sup>

<sup>1</sup>Molecular Science Institute, Universitat de València, Apartado 22085, Valencia ES-46071, Spain

<sup>2</sup>Institute of Organic and Pharmaceutical Chemistry, National Hellenic Research Foundation, 48 Vas. Constaninou Ave., Athens 116 35, Greece

<sup>3</sup>Department of Informatics and Computer Technology, Lamia Institute of Technology, 35100, Lamia, Greece

<sup>4</sup>Accelrys Inc., Telesis Court, San Diego, California 92121, USA

<sup>5</sup>Université de Pau et des Pays de l'Adour-IPREM, ECP-UMR CNRS 5254, Helioparc, 2 av. du président Angot, Pau Cedex 09 64053, France

<sup>6</sup>Department of Physical and Theoretical Chemistry, Faculty of Natural Sciences, Comenius University, Mlynská Dolina, Bratislava SK-842-15, Slovakia

(Received 29 June 2009; accepted 7 September 2009; published online 7 October 2009)

Some linear and nonlinear optical (NLO) properties of Ni(SCH)<sub>4</sub> and several of its derivatives have been computed by employing a series of basis sets and a hierarchy of methods (e.g., HF, DFT, coupled cluster, and multiconfigurational techniques). The electronic structure of Ni(SCH)<sub>4</sub> has been also analyzed by using CASSCF/CASPT2, *ab initio* valence bond, and DFT methods. In particular we discuss how the diradicaloid character (DC) of Ni(SCH)<sub>4</sub> significantly affects its NLO properties. The quasidegeneracy of the two lowest-energy singlet states  $1^1A_g$  and  $1^1B_{1u}$ , the clear DC nature of the former, and the very large number of low-lying states enhance the NLO properties values. These particular features are used to interpret the NLO properties of Ni(SCH)<sub>4</sub>. The DC of the considered derivatives has been estimated and correlated with the NLO properties. CASVB computations have shown that the structures with Ni(II) are the dominant ones, while those with Ni(0) and Ni(IV) have negligible weight. The weights of the four diradical structures were discussed in connection with the weight of the structures, where all the electrons are paired. Comparative discussion of the properties of Ni(SCH)<sub>4</sub> with those of tetrathia fulvalene demonstrates the very large effect of Ni on the properties of the Ni-dithiolene derivatives. A similar remarkable effect on the NLO properties is produced by one or two methyl or C<sub>3</sub>S groups. The considered Ni-dithiolene derivatives have exceptionally large NLO properties. This feature in connection with their other physical properties makes them ideal candidates for photonic applications. © 2009 American Institute of Physics. [doi:10.1063/1.3238234]

### I. INTRODUCTION

There is currently a great interest in photonic materials, since they have a large number of important applications, for example, they can be used to construct devices for all optical switching, optical communications, data storage, signal processing, and optical limiting.<sup>1,2</sup> One of the specific needs, related to the above applications, is to develop derivatives, which have nonlinear optical properties several orders of magnitude larger than those which are currently available. Experimental and theoretical evidence suggests that metal dithiolenes is a very promising class of materials.<sup>3–5</sup> This is due to the extensive  $\pi$ -electron delocalization and the low lying excited states. Ni bis(dithiolene) complexes have several other attractive features:<sup>6</sup> (i) photochemical and thermal stability, (ii) reversible and widely tunable properties, and (iii) they are very suitable for *Q*-switching lasers.<sup>7</sup> These derivatives have been considered for various other important

applications, e.g., molecular magnets, conductors, and superconductors.<sup>8–10</sup> In addition, the electronic structure of nickel dithiolenes is of great interest and many research teams contributed to the elucidation of their structures in the past 50 years.<sup>11,12</sup>

In this work we consider the linear and nonlinear optical (L&NLO) properties of bis(ethylene)-1,2-dithiolato nickel or NiBDT [Ni(S<sub>2</sub>C<sub>2</sub>H<sub>2</sub>)<sub>2</sub> or Ni(SCH)<sub>4</sub>] and some of its derivatives (Fig. 1). There are several experimental studies on the NLO properties of metal dithiolene complexes.<sup>13–17</sup> However, there are only few theoretical studies on the NLO properties of Ni dithiolenes.<sup>12,18–20</sup>

In this work we will first study the electronic structure of NiBDT employing a series of methods: CASSCF/CASPT2, *ab initio* VB, and DFT. Each one of them provides some distinct piece of information and all of them contribute to complete the puzzle of the electronic structure of NiBDT. This information is used to interpret the L&NLO properties of the selected dithiolenes. More specifically this work has three objectives:

<sup>a)</sup>Authors to whom correspondence should be addressed. Electronic addresses: luis.serrano@uv.es, aavram@eie.gr, and mpapad@eie.gr.

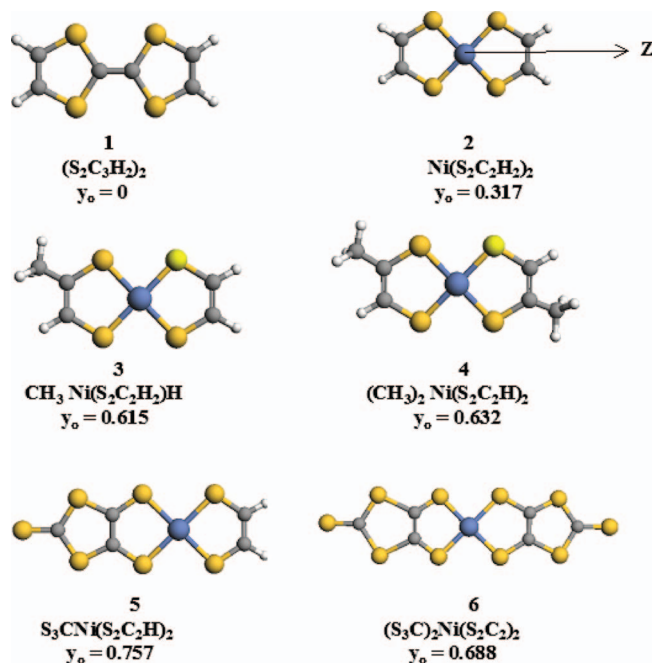


FIG. 1. The structures of the TTF (1) and some Ni-dithiolenes (2–6). The parameter  $y_0$ , estimating the DC, is also given (see text).

- To elucidate the structure of NiBDT. Three state-of-the-art techniques have been used and each one of them provides complementary information to the other ones. Of particular importance is the singlet-diradical character of NiBDT, which is studied by employing various criteria.
- To perform a detailed and systematic study of the L&NLO properties of NiBDT, employing various methods (e.g., CASSCF/CASPT2, a series of functionals, etc.) in order to find the most appropriate technique for the computation of the properties of interest of the chosen series of derivatives. It is of interest to discuss the large effect of the structural changes of NiBDT on the NLO properties.
- To employ the electronic structure information in order to interpret the L&NLO properties of the considered derivatives.

The work is organized as follows. In Sec. II we briefly present the recent relevant work on the diradical character (DC) and how it has been used to interpret the NLO properties. In the Sec. III we present the computational techniques we used. Section IV involves the discussion of our results and finally in Sec. V we present our concluding remarks.

## II. DIRADICAL CHARACTER

Salem and Rowland in their pioneering work noted that the term *diradical* can be used to describe loosely derivatives with two unpaired electrons.<sup>21</sup> Wirz<sup>22</sup> suggested that a diradical is “a molecular entity whose lowest singlet and triplet state energies do not differ by much more than  $kT$ , say 2 kcal mol<sup>-1</sup>. The expression ‘biradicaloid’ would then extend this range to say 24 kcal mol<sup>-1</sup>. ” Alternatively one may define the diradical as a system with the singly occupied

orbitals, separated enough to make the resulting singlet ( $S$ ) and triplet ( $T$ ) states degenerate or nearly degenerate.

It has been noted that “The term diradical has generally been used loosely to describe systems which can be formally written with two unpaired electrons.”<sup>21</sup> In Sec. IV we will discuss some criteria for the evaluation of the DC of NiBDT. Here we will briefly review some recent relevant work on DC.

The singlet DC of species such as  $M^{IV}(L^{2-})_2$ , where  $M = \text{Cr, Mo, W}$ , and  $L$  is a tridentate azoaromatic ligand, has been studied by employing structural, magnetic, redox, and spectroscopic data as well as DFT calculations (B3LYP, PB0). Sanyal *et al.*<sup>23</sup> used a broken-symmetry (BS) approach,<sup>24</sup> in the framework of DFT, to study their singlet diradicals. It has been shown that intramolecular, antiferromagnetic coupling of two  $\pi$  radicals leads to a diamagnetic ground state ( $S=0$ ).<sup>23</sup>

The spectroscopy oriented configuration interaction (SORCI) technique has been employed by Ray *et al.*<sup>25</sup> to study the electronic properties of  $[M^{II}(L)_2]$ ,  $M = \text{Ni, Pd, Pt}$ . These square planar diamagnetic compounds involve two S,S-coordinated 1,2-dithiosemiquinonate(-1)  $\pi$  radical anions. It has been noted that there is a strong antiferromagnetic coupling of the two spins. The diamagnetic metal(II) ion ( $nd^8$ ,  $S_m=0$ ) is involved in the above intramolecular mechanism. The singlet DC depends on the metal (Ni: 32%, Pd: 50%, Pt: 30%). Ray *et al.*<sup>25</sup> make two important comments: (i) the value of the DC depends strongly on the theoretical method and (ii) DC is not a physical observable. However, DC allows discussion of changes and trends in a series of compounds. In addition, it provides a tool to rationalize the open-shell character of the investigated systems.

The [Cu–P–Cu–P] diamandoids have been studied by Rhee and Head-Gordon. They found that a singlet diradicaloid species is formed by two spatially separated, and thus partially unpaired electrons.<sup>26</sup> They noted that a singlet diradicaloid is due to partial electron occupation of the antibonding orbitals.<sup>21</sup> It has been noted that diradicaloids may be used to rationalize intermediates and transition states and to develop novel materials (e.g., spintronics and molecular ferromagnets).<sup>26</sup>

Thomas *et al.*<sup>27</sup> studied a series of diradicaloid croconate dyes with DFT techniques. They found that broken symmetry-UDFT highest occupied molecular orbital (HOMO)-lowest unoccupied molecular orbital (LUMO) gaps are overestimated due to spin contamination. Prabhakar *et al.*<sup>28</sup> prepared a series of croconate dyes. They found that decrease in the HOMO-LUMO gap is associated with increase in the singlet DC. It has been shown that there is a correlation of the DC to the near-IR absorption.<sup>29</sup>

Bachler *et al.*<sup>30</sup> used DFT and CASSCF computations to discuss the DC of a series of square planar, diamagnetic complexes. They noted that (i) DC of the considered complexes suggests the presence of Ni(II) and (ii) “The singlet diradical character of a molecule should be large provided the symmetry broken unrestricted DFT for the electronic ground state is much lower in energy than the energy of the restricted singlet ground-state DFT solution.”

Fukui *et al.*<sup>12</sup> used hybrid DFT to investigate the depen-

dence of the second hyperpolarizability on DC of a series of square planar nickel complexes, which involve several types of bidentate ligands:  $o\text{-C}_6\text{H}_4\text{XY}$ , where  $X=Y=\text{O}$ ,  $\text{NH}$ ,  $\text{S}$ ,  $\text{Se}$ ,  $\text{PH}$ , and  $(X, Y)=(\text{NH}, \text{NH}_2)$  and  $(\text{S}, \text{NH}_2)$ . They found that the largest second hyperpolarizability values are associated with intermediate DC. Nakano and co-workers also discussed the effect of the DC on the second hyperpolarizabilities<sup>31–36</sup>

Prabhakar *et al.*<sup>28</sup> synthesized a series of croconate dye derivatives with aniline and substituted anilines as donors to axially group. They found large second nonresonant hyperpolarizability values ( $-4.76$  to  $-10.52 \times 10^7$  a.u.), employing degenerate four wave-mixing experiments. They suggested that DC in croconates has a major contribution in these large values, and not the donor groups.

Finally, Yesudas and Bhanuprakash<sup>37</sup> investigated the second hyperpolarizability of some oxallyl diradicaloids, employing a series of methods (e.g., DFT, a symmetry adapted cluster configuration interaction method). They suggested that the large second hyperpolarizabilities are due to a mixture of intermediate DC, some zwitterionic character, and a large coupling between these two valence bond (VB) forms.

### III. COMPUTATIONAL METHODS

When a molecule is set in a uniform static electric field  $F$ , its energy,  $E$ , may be expanded as follows:<sup>38</sup>

$$E = E^0 - \mu_i F_i - (1/2)\alpha_{ij} F_i F_j - (1/6)\beta_{ijk} F_i F_j F_k - (1/24)\gamma_{ijkl} F_i F_j F_k F_l - \dots, \quad (1)$$

where  $E^0$  is the field free energy of the atom or the molecular system,  $F_i$ ,  $F_j$ ,  $F_k$ , and  $F_l$  are the field components, and  $\mu_i$ ,  $\alpha_{ij}$ ,  $\beta_{ijk}$ , and  $\gamma_{ijkl}$  are the tensor components of the dipole moment, linear dipole polarizability, and first and second hyperpolarizability, respectively. Summation over repeated indices is implied. A finite field approach using Eq. (1) was employed to compute  $\alpha_{zz}$  and  $\gamma_{zzzz}$  of the derivatives of interest.

All the geometries used in this study were optimized at the B3LYP (Ref. 39) level of approximation, since this method is known to provide satisfactory geometries for diradical systems.<sup>40,41</sup> This is defined as procedure A. However, in order to check that the above approach is satisfactory, we used procedure B for NiBDT, which involves the following two steps: (i) the structure of the triplet state of NiBDT has been optimized with UB3LYP and (ii) the resulting geometry (from the first step) was used as starting point to optimize the structure of the singlet using the BS UB3LYP approach (guess=mix option in Gaussian).<sup>42–44</sup> Both procedures A and B gave similar molecular geometries. This observation is in agreement with the finding of Bachler *et al.*,<sup>30</sup> who used RDFT and obtained satisfactory results (in comparison with the experimental ones) for the molecules they considered. Thus, the DC was neglected in the geometry optimization. The computed adiabatic singlet (BS-UB3LYP) and triplet (UB3LYP) energy gap is  $-9.91$  kcal mol<sup>-1</sup>, an indication of the diradicaloid character of NiBDT. It is noted that the singlet is of lower energy. For Ni a quasirelativistic effective core pseudopotential was employed [ECP28MWB

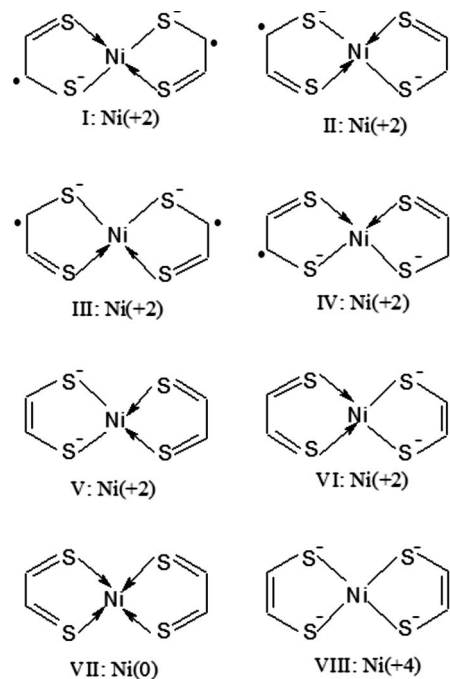


FIG. 2. The resonance structures of NiBDT, according to VB computations.

(SDD)],<sup>45</sup> whereas for C, S, and H, the 6-31G\* basis set series was used. All the optimized molecular structures lie on the  $xz$  plane and their longitudinal axis is oriented along the  $z$ -direction. NiBDT, at the ground state, belongs to the  $D_{2h}$  point group.

VB calculations with localization enhanced VB orbitals have been performed for  $\text{Ni}(\text{SCH})_4$ , using the VB2000 program.<sup>46,47</sup> All electrons are included in calculations. Since the complex has nine heavy atoms, a modest basis set of 6-31G, which corresponds to 125 basis functions for this compound, is used for the VB calculations. All 14 valence  $\pi$  electrons, which include ten electrons from the two ligands and four electrons from the two 3d orbitals of Ni, were included in the VB treatment and the remaining electrons were treated at the Hartree–Fock level. Eight resonance structures, which are shown in Fig. 2, are used in the calculations. The 11 VB orbitals, describing the eight resonance structures, are optimized for the total energy of the system. VB calculations usually return highly localized nonorthogonal orbitals, therefore the structure weight analysis based on high quality VB wave functions is more meaningful than that based on popular natural resonance theory.<sup>48</sup> In order to enhance even more the localization of VB orbitals, the algorithm developed by Li *et al.* has been used.<sup>47</sup> Three different methods<sup>49–51</sup> for determining the weights of the eight resonance structures have been used. These have been proposed by Mulliken, Löwdin, and Hiberty. All three methods give similar results, which will be discussed in the next section.

The excitation energies of 16 excited states of NiBDT have been computed by employing the CASSCF/CASPT2 method in its zeroth-order Hamiltonian form<sup>52</sup> and the all-electron relativistic ANO-RCC  $\text{Ni}[6s5p3d1f]/\text{S}[5s4p2d]/\text{C}[4s3p1d]/\text{H}[2s1p]$  one-electron basis set.<sup>53</sup> An active space of 12 electrons distributed in 12 molecular orbitals (MOs) was employed to obtain excitation energies, oscillator

strengths, and wave functions. Inner core electron were frozen in the perturbative step. Scalar relativistic effects were included using the Douglas–Kroll approach.<sup>54–56</sup>

The L&NLO properties were computed by employing a series of techniques including density functional theory, restricted (RHF) and unrestricted symmetry-broken Hartree-Fock solutions (UHF), spin-projected UHF (PUHF),<sup>57</sup> UCCSD,<sup>57</sup> UCCSD(T),<sup>57</sup> in which a perturbative treatment of triples is included, and CASSCF/CASPT2 or RASSCF/RASPT2, with the use of the multistate option (MS-CASPT2 or MS-RASPT2).<sup>53,58,59</sup>

The density functional theory has been applied by employing the following functionals: (i) B3LYP,<sup>39</sup> (ii) BHandHLYP,<sup>60</sup> and (iii) the double-hybrid functional UB2-PLYP.<sup>61</sup> The (U)BHandHLYP functional includes 50% Hartree–Fock exchange and was used by Fukui *et al.*<sup>12</sup> to get reasonable second hyperpolarizability values for a series of singlet diradical square-planar nickel complexes. The UB2-PLYP functional, on the other hand, mixes standard generalized gradient approximations for exchange, proposed by Becke (B),<sup>62</sup> the method of Lee, Young and Parr (LYP) (Ref. 60) for correlation, Hartree–Fock exchange (53%), and a MP2 correlation contribution (27%).

The ZPolX basis sets developed by Benkova *et al.*<sup>63,64</sup> for first- and second-row atoms and Baranowska *et al.*<sup>65</sup> for first-row transition metals have been used in the computation of the L&NLO properties. The acronym ZPolX, where X is the element symbol, is equivalent to Z3PolX used in early papers<sup>63,64</sup> on the basis set generation. Moreover, in order to check the basis set effect, the aug-cc-pVnZ, series,  $n = D, T, Q$ ,<sup>66–70</sup> was employed in connection with the UBHandHLYP method. For Ni (10) an effective core potential was used.<sup>45</sup> In parentheses the number of core electrons is denoted. Only the longitudinal components of the polarizability ( $\alpha_{zz}$ ) and second hyperpolarizability tensor ( $\gamma_{zzzz}$ ) were computed. These are the dominant components and they are adequate for the purposes of the present work.

All the property values were computed by employing the Romberg approach, in order to remove higher order contaminations.<sup>71</sup> A number of field strengths of the magnitude  $2^m F$ , where  $m=1,2,3,4$  and a base field ( $F$ ) of 0.001 a.u. (and 0.005 a.u., for the CASSCF/CASPT2) were used. The GAUSSIAN 03 software<sup>72</sup> has been employed for the UDFT and UCCSD(T) calculations, while for the CASSCF/CASPT2 and the RCCSD/RCCSD(T) computations the MOLCAS-7 suite of programs was used.<sup>53</sup>

## IV. RESULTS

In this section we will consider: (i) the electronic structure of NiBDT and how this can be used to rationalize its second hyperpolarizability, (ii) a series of criteria for the evaluation of the DC, which is of cardinal importance for the response properties of the Ni dithiolene derivatives, (iii) the L&NLO properties of NiBDT, and (iv) the effect of changes in the structure on the L&NLO properties.

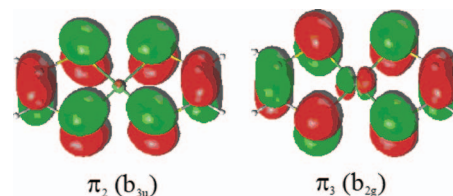


FIG. 3. CASSCF  $\pi$  orbitals in which two electrons, forming the singlet biradical, are placed in NiBDT.

### A. The electronic structure of NiBDT

NiBDT,  $\text{Ni}(\text{S}_2\text{C}_2\text{H}_2)_2$ , or bisdithioglyoxalnickel,<sup>73</sup> is a characteristic example of square planar derivatives, which involve conjugated ligands with sulfur. Several bonding structures have been proposed for NiBDT.<sup>11,19</sup> These involve 8, 10, or 12  $\pi$  electrons (Figs. 2 and 3). The formal oxidation state of Ni is 0, +2, and +4, respectively. For  $\text{Ni}^0$ , the ligands retain their dithioketonic structure, but there is no evidence that such a complex exists.<sup>74</sup> For  $\text{Ni}^4$ , the ligands are assumed to be dithiolatodians,  $^-\text{S}-\text{CH}=\text{CH}-\text{S}^-$ . It has been pointed out that such dianions are absent in  $d^8$  neutral  $\text{Ni}(\text{S}_2\text{C}_2\text{H}_2)_2$ .<sup>74</sup>

Evidence from proton magnetic resonance spectra and infrared C–S and C–C stretching frequencies strongly suggest the adoption of the 10  $\pi$  electron system,<sup>11</sup> for which two models have been proposed. (i) The first model involves the resonance structures V and VI (Fig. 2), originally proposed by Bach and Hohm.<sup>75</sup> The positive charge of Ni ( $d^8$ ) is counterbalanced by the two negative charges in one of the ligands. The neutral ligand (dithioglyoxal) has 4  $\pi$  electrons and the dianion 6  $\pi$  electrons (dithiolate).<sup>76</sup> It has been proposed that this structure accounts for 87% of the ground state description,<sup>11</sup> and (ii) the second model involves the singlet diradical resonance structures (structures I–IV; Fig. 2) suggested by Stiefel *et al.*<sup>77</sup> For completeness we note that our recent vibrational analysis of NiBDT, based on DFT results, is more consistent with structure IV, although structures II–V cannot be excluded. These results will be presented in another publication.

Bachler *et al.*<sup>30</sup> noted that there is a significant difference in the MO description provided by these two models. A singlet diradical involves two singly occupied MOs of equal energy, where the two electrons have opposite spin and are weakly antiferromagnetically coupled. On the contrary the closed shell description involves a single HOMO, occupied by two electrons with antiparallel spin, which occupy the same region in space. The experimental distinction between a singlet diradical and a closed shell is a difficult problem, since both compounds are diamagnetic even at room temperature.

It has been noted that a single determinant wave function cannot properly describe a singlet diradical. This means that HF and DFT techniques could be insufficient.<sup>30</sup> A multiconfigurational wave function can treat the static correlation required for the proper description of singlet diradicals. Up to certain extent the unrestricted Hartree–Fock can also give a reasonable description of the static correlation.

In the following paragraphs, we will consider the elec-

TABLE I. Excited states structure of NiBDT at the diradical optimized structure. The computations have been performed by employing the CASSCF/CASPT2 method.

State	$\Delta E/\text{eV}$	Main configuration
$1^1A_g$ (diradicaloid) <sup>a</sup>	-0.004 <sup>b</sup>	$\cdots(\pi_2)^2(\pi_3)^0 - (\pi_2)^0(\pi_3)^2$
$1^1B_{1u}$ ( $\pi\pi^*$ ) <sup>c</sup>	0.000 <sup>b</sup>	$\cdots(\pi_2)^1(\pi_3)^1$
$1^1B_{2g}$ ( $\sigma_{\text{SNI}}\pi^*$ )	0.563	$\cdots(\sigma_{\text{SNI}})^1(\pi_2)^2(\pi_3)^1$
$1^1A_u$ ( $\sigma_{\text{SNI}}\pi^*$ )	0.740	$\cdots(\sigma_{\text{SNI}})^1(\pi_2)^2(\pi_3)^1$
$1^1B_{3g}$ ( $\pi\pi^*$ )	0.891	$\cdots(\pi_1)^1(\pi_2)^2(\pi_3)^1$
$2^1A_u$ ( $\pi\sigma_{\text{CSNI}}^*$ )	0.999	$\cdots(\pi_2)^1(\pi_3)^0(\sigma_{\text{CSNI}}^*)^1$
$1^1B_{1g}$ ( $\sigma_{\text{SNI}}\pi^*$ )	1.592	$\cdots(\sigma_{\text{SNI}})^1(\pi_2)^2(\pi_3)^1$
$1^1B_{3u}$ ( $\sigma_{\text{SNI}}\pi^*$ )	1.672	$\cdots(\sigma_{\text{SNI}})^1(\pi_2)^1(\pi_3)^2$
$1^1B_{2u}$ ( $\pi\pi^*$ )	1.785	$\cdots(\pi_1)^1(\pi_2)^1(\pi_3)^2$
$2^1B_{2u}$ ( $\sigma_{\text{SNI}}\sigma_{\text{CSNI}}^*$ )	2.078	$\cdots(\sigma_{\text{SNI}})^1(\pi_2)^1(\pi_3)^1(\sigma_{\text{CSNI}}^*)^1$
$2^1A_g$ ( $\pi\pi^*$ )	2.120	$\cdots(\pi_2)^2(\pi_3)^0 + (\pi_2)^0(\pi_3)^2$
$2^1B_{3u}$ ( $\sigma_{\text{SNI}}\sigma_{\text{CSNI}}^*$ )	2.170	$\cdots(\sigma_{\text{SNI}})^1(\pi_2)^1(\pi_3)^1(\sigma_{\text{CSNI}}^*)^1$
$2^1B_{1g}$ ( $\sigma_{\text{SNI}}\sigma_{\text{CSNI}}^*$ )	2.680	$\cdots(\sigma_{\text{SNI}})^1(\pi_2)^1(\pi_3)^1(\sigma_{\text{CSNI}}^*)^1$
$2^1B_{2u}$ ( $\sigma_{\text{SNI}}\sigma_{\text{CSNI}}^*$ )	2.735	$\cdots(\sigma_{\text{SNI}})^1(\pi_2)^1(\pi_3)^1(\sigma_{\text{CSNI}}^*)^1$
$3^1A_u$ ( $\sigma_{\text{SNI}}\pi^*$ )	2.774	$\cdots(\sigma_{\text{SNI}})^1(\pi_2)^1(\pi_3)^2$
$2^1B_{2g}$ ( $\pi\pi\pi^*\sigma_{\text{CSNI}}^*$ )	2.995	$\cdots(\pi_1)^1(\pi_2)^2(\pi_3)^0(\sigma_{\text{CSNI}}^*)^1$
$3^1B_{3u}$ ( $\sigma_{\text{SNI}}\pi\pi^*\pi^*$ )	3.064	$\cdots(\sigma_{\text{SNI}})^1(\pi_1)^1(\pi_2)^2(\pi_3)^2$
$1^3B_{1u}$ (diradical) <sup>d</sup>	0.612	$\cdots(\pi_2)^1(\pi_3)^1$

<sup>a</sup>  $1^1A_g$  [71% $(\pi_2)^2(\pi_3)^0 - 21\%(\pi_2)^0(\pi_3)^2$ ].

<sup>b</sup> The energy difference is within the method accuracy. For simplicity the  $1^1A_g$  state will be considered the ground state at this level.

<sup>c</sup>  $1^1B_{1u}$  state 65% [ $(\pi_2)^1(\pi_3)^1$ ].

<sup>d</sup>  $1^3B_{1u}$  state 92% [ $(\pi_2)^1(\pi_3)^1$ ].

tronic structure of NiBDT by employing three different approaches: (i) CASSCF/CASPT2 computations, (ii) CASVB computations, and (iii) DFT calculations.

**CASSCF/CASPT2 computations.** The results on Table I describe the excited states structure of NiBDT (at the ground state DFT BS geometry) computed at the CASPT2 level using the ANO-RCC Ni[6s5p3d1f]/S[5s4p2d]/C[4s3p1d]/H[2s1p] basis set. In order to build the basic active space for NiBDT, we need to include at least the highest- and lowest-lying pairs of  $\pi$  orbitals, two  $\pi$  and two  $\pi^*$ , and the four bonding and four antibonding orbitals of the weak and large Ni-S bonds. This initial active space involves therefore 12 electrons and 12 MOs, labeled as 12/4242 ( $4\sigma 2\pi 4\sigma^* 2\pi^*$ ), including the number of active electrons (12) and the number of MOs in the subspaces of  $C_{2v}$  symmetry ( $a_1b_1b_2a_2$ ). The same active space was employed for the calculation of the electronic spectra in the subspaces of the  $D_{2h}$  point group, that is, 12/(21212121), following the labeling: number of electrons/( $a_g b_{1u} b_{2g} b_{3g} b_{1g} b_{2u} b_{3u} a_u$ ).

The main finding of the CASSCF/CASPT2 computations is the quasidegeneracy of  $1^1B_{1u}$  and  $1^1A_g$  states and the large number of low-lying excited states of NiBDT. These features suggest that NiBDT is very likely to have large NLO properties.<sup>78</sup> Two singlet states have been computed as quasidegenerate at the CASPT2 level (4 meV) at the planar optimized  $D_{2h}$  geometry, the  $1^1B_{1u}$  [65% $(b_{3u})^1(b_{2g})^1$ ] and  $1^1A_g$  [71% $(b_{3u})^2(b_{2g})^0 - 21\%(b_{3u})^0(b_{2g})^2$ ] states. Such value is within the expected accuracy of the method, therefore we cannot establish conclusively which one is the ground state. For the sake of simplicity the  $1^1A_g$  state will be then considered the ground state at this geometry

CASSCF natural occupation numbers for the  $1^1B_{1u}$  state indicate that almost one electron (actually 1.18 and 0.84) is placed in each of the  $b_{3u}$  and  $b_{2g}$  orbitals (Fig. 3). For  $1^1A_g$  the natural occupations are 1.54 and 0.48, respectively, for the same MOs, a consequence of the large weight of the double excited closed-shell configuration. According to Salem and Rowland<sup>21</sup> the degree of DC is related to twice the weight of double excitation configuration in the ground state configuration. Here it reaches 42%, a clear illustration of the diradicaloid character of the system. As observed below in the CASVB results, the charge on the Ni is close to +2 in the low lying states. The presence of the nickel atom has the twofold consequence: it leads to the degeneracy of the  $\pi$  orbitals and it weakens the  $\sigma$  bonding structure. Excitations involving the S-Ni  $\sigma$  bonds are accessible from 0.563 eV, whereas  $\sigma^*$  antibonding orbitals with C-S-Ni contributions are also present at low energies (see Table I). As compared with TTF (tetrathiafulvalene; Fig. 1), in which one single  $\pi\sigma^*$  transition was present below 3 eV,<sup>79</sup> the NiBDT molecule displays no less than 16 states in the range of the visible spectrum. In TTF, the ‘‘HOMO-like’’ and ‘‘LUMO-like’’  $\pi$  MOs are not degenerate. In NiBDT, they almost are ( $b_{3u}$  and  $b_{2g}$ ), containing one electron each leading to the quasidegeneracy structure. The Ni atom in Ni(SCH)<sub>4</sub> is basically closed-shell, having very long sigma-type bonds with sulfur. Those are much longer than the C-S bonds in TTF and therefore weaker. This is why there are so many low-lying  $\sigma-\pi^*$  and  $\pi-\sigma^*$  excitations at low energies which enhance the NLO properties.

Another indication of the nature of the lowest-energy states of the molecule can be obtained from the calculation of the lowest triplet state  $1^3B_{1u}$ . Computed at 0.608 eV above the singlet  $1^1A_g$  ground state, the triplet structure is actually that of a pure diradical, displaying natural occupation numbers 1.00 for both the  $b_{3u}$  and  $b_{2g}$  MOs and a wave function contribution of 92% for the configuration  $(b_{3u})^1(b_{2g})^1$ , as compared with and the covalent-ionic  $1^1A_g$  [71% $(b_{3u})^2(b_{2g})^0 - 21\%(b_{3u})^0(b_{2g})^2$ ] and the ionic  $1^1B_{1u}$  (65% $[(b_{3u})^1(b_{2g})^1]$ ) states. This description and the fact that the singlet-triplet gap is not zero lead to characterize the ground-state complex as having diradicaloid, not diradical, character. A small positive singlet-triplet gap, strongly dependent on the molecular geometry, is also typical of the diradicaloid systems.<sup>44</sup> Breaking the planarity of the system makes both the lowest singlet and triplet states become degenerate, and therefore the system becomes a pure diradical at a twisted (butterflylike) 20° angle (see Fig. 4).

**Ab initio VB computations.** The structure weights (Table II) have been computed with three different methods reported by Chirgwin-Coulson<sup>49</sup> (which is also called Mulliken method in the VB2000 program), Löwdin,<sup>50</sup> and Hiberty.<sup>51</sup> All three different methods give quite similar results. The consistency of the three different structure weight methods indicates that there is little ambiguity about the computed structure weights in this system. We observe that the first two diradical structures (I, II) have considerably larger weight than III and IV. The relatively closer distance of the radical centers of the latter pair in comparison with the former is likely to destabilize the structures and to lead to lower

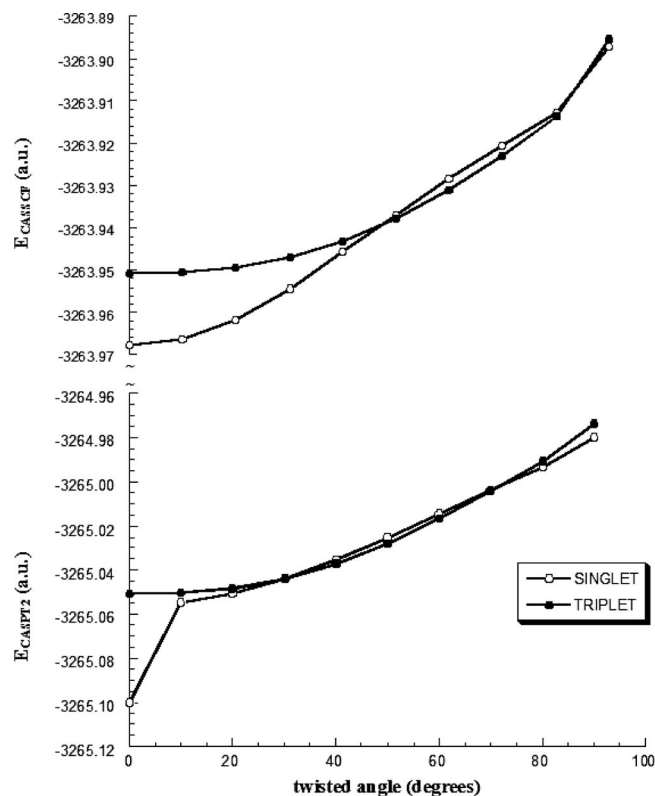


FIG. 4. The CASSF and CASPT2 energies of Ni(S<sub>2</sub>C<sub>2</sub>H<sub>2</sub>)<sub>2</sub> as a function of the twist angle. The moiety S<sub>2</sub>C<sub>2</sub>H<sub>2</sub> is rotated around the z axis (Fig. 1).

weights. This is also shown by the lower energy of I/II in comparison to that III/IV (Table III). In structures V and VI, all electrons are paired and this may contribute to their higher stability, in comparison with the other four structures I–IV. Structure VII[Ni(0)] has negligible weight and structure VIII[Ni(+4)] has zero weight, with which is associated the higher energy.

**DFT computations.** It has been observed that the restricted DFT solution of NiBDT is unstable, thus a broken symmetry BS-(U)DFT solution has been found. The guess =mix option in GAUSSIAN (Refs. 42–44) has been used to verify the symmetry broken solution, starting from the restricted solution. For a singlet diradical, the symmetry broken solution gives Kohn–Sham (KS) spin orbitals, which have different space parts for  $\alpha$  and  $\beta$  electrons. In Fig. 5 we observe the magnetic orbitals for NiBDT. Bachler *et al.*<sup>30</sup> noted that “If we cannot find an occupied  $\beta$  orbital that matches the shape of an  $\alpha$  orbital, the KS orbital is a magnetic orbital.” Figure 5 describes the HOMO  $\alpha$  and  $\beta$  electrons of NiBDT and TTF. In the latter there is a match of the

TABLE III. Energy of resonance structures (Fig. 2). All values are in a.u. (conversion factors for energy units: 1 hartree  $\approx$  27.210 70 eV  $\approx$  627.51 kcal mol<sup>-1</sup>  $\approx$  219 474.6 cm<sup>-1</sup>)

Structure	Energy	Structure	Energy
I	-3250.127 68	V	-3250.172 55
II	-3250.127 68	VI	-3250.172 55
III	-3250.081 35	VII	-3249.779 55
IV	-3250.081 35	VIII	-3248.921 54

shapes of the  $\alpha$  and  $\beta$  MOs and strong antiferromagnetic coupling, while in NiBDT, the  $\alpha$  and  $\beta$  orbitals are weakly antiferromagnetically coupled (magnetic orbitals).

## B. Criteria for the evaluation of the diradical character

One may use several criteria to evaluate the DC. First, we may use the difference<sup>29</sup>

$$E_1 = E_{\text{UDFT}}(\text{singlet}) - E_{\text{RDFT}}(\text{singlet}). \quad (2)$$

The above energy difference is denoted by  $E_1$  and gives the energy lowering, which results by employing the symmetry broken DFT solutions in comparison with the values given by RDFT. This arises from spin decoupling, which has the tendency to localize the electrons in different parts of the molecule. The singlet DC is associated with the energy lowering caused by the BS solution, which simulates the static electron correlation.<sup>30</sup>  $E_1$  for NiBDT is  $-0.0507$  kcal mol<sup>-1</sup>. Srinivas *et al.*<sup>29</sup> also noted that most of the squaraines they considered are associated with  $E_1$  close to zero. A large DC may be associated with a large  $E_1$  value.

Another criterion is the singlet-triplet gap as defined by Srinivas *et al.*:<sup>29</sup>

$$E_2 = E_{\text{UDFT}}(\text{triplet}) - E_{\text{RDFT}}(\text{singlet}), \quad (3)$$

$E_2$  for NiBDT is 9.27 kcal mol<sup>-1</sup>. According to the definition of Wirtz<sup>22</sup> for diradicals and diradicaloids, NiBDT should belong to the class of diradicaloids.  $E_2$  may be interpreted as the energy required to invert one spin. Thus a small  $E_2$  value indicates a large DC.<sup>21,30</sup>

Other authors used the following expression for the singlet-triplet energy gap:<sup>30,43,80</sup>

$$E_{st} = E_s - E_t = \frac{2(E(b) - E_u)}{2 - (\langle \Psi(b) | S^2 | \Psi(b) \rangle)}, \quad (4)$$

where  $E_s$  and  $E_t$  are the energies of the singlet and triplet state, respectively;  $E(b)$  is the energy of the symmetry broken state (UDFT) and  $E_u$  is the energy (UDFT) of the high spin triplet state.  $\Psi(b)$  is the symmetry broken KS Slater

TABLE II. Weights of eight resonance structures of VB calculations for NiBDT (Fig. 2).

Method	Structure weight							
	I	II	III	IV	V	VI	VII	VIII
Mulliken	0.1945	0.1945	0.1162	0.1162	0.1864	0.1864	0.0060	0.0000
Löwdin	0.1815	0.1815	0.1122	0.1122	0.2014	0.2014	0.0099	0.0000
Hiberty	0.2049	0.2049	0.1042	0.1042	0.1902	0.1902	0.0014	0.0000

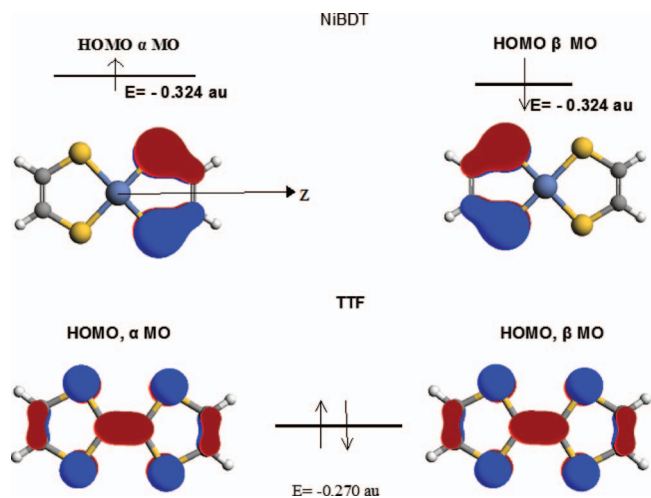


FIG. 5. The  $\alpha$  and  $\beta$  spin HOMOs of NiBDT and TTF, computed by the UHF method.

determinant and  $\langle \Psi(b) | S^2 | \Psi(b) \rangle$  is the total spin expectation value. The value of  $\langle \Psi(b) | S^2 | \Psi(b) \rangle$  reflects the spin polarization of the inner closed shells computed by the symmetry broken KS Slater determinant. Bachler *et al.*<sup>30</sup> noted that the symmetry broken wave function involves singlet and triplet wave functions with similar weights, if  $E_{st}$  in a singlet diradical is small. We found that  $E_{st}$  is  $-9.91$  kcal mol<sup>-1</sup> for NiBDT. Both  $E_2$  and  $E_{st}$  are in reasonable agreement. An extensive discussion of the singlet-triplet energy gap and the various formulae presented to evaluate it are given by Bachler *et al.*<sup>30</sup> These authors studied the DC of a series of square planar Ni derivatives and found that  $E_{st}$  [computed by Eq. (4)] gets values from 4.4 to 11.1 kcal mol<sup>-1</sup>. On the other hand, the CASPT2 energy values also confirm the positive singlet-triplet energy gap and therefore the diradicaloid nature of the  $D_{2h}$  system and the degeneracy of the lowest singlet and triplet states of the bent molecule (see Fig. 4), which has therefore a DC.

Fukui *et al.*<sup>12</sup> used the parameter  $y_i$ , associated with HOMO- $i$  and LUMO+ $i$ , where HOMO is the highest occupied molecular orbital and LUMO is the lowest unoccupied molecular orbital, to estimate the DC. This is defined by the weight of the doubly excited configuration in the multiconfiguration SCF method and in the spin projected UHF (PUHF) theory is given by<sup>81,82</sup>

$$y_i = 1 - \frac{2T_i}{1 + T_i^2}, \quad (5)$$

where  $T_i$  is the orbital overlap between the corresponding orbital pairs and can be expressed using the occupation numbers ( $n_i$ ) of UHF natural orbitals:

$$T_i = \frac{n_{\text{HOMO}-i} - n_{\text{LUMO}+i}}{2}. \quad (6)$$

The parameter  $y_i$  varies from 0 (closed shell; 0% DC) to 1 (pure diradical; 100% DC). In this study we use the HOMO and LUMO ( $y_0$ ). According to this criterion NiBDT has intermediate DC, while compounds 3–6 (Fig. 1) have high DC. If natural occupation numbers for the corresponding

TABLE IV. A Basis set study of NiBDT (the B3LYP/SDD optimized geometry was employed to all calculations). The UBHandB3LYP functional was employed. All values are in a.u.

Basis set	Property	
	$\alpha_{zz}$	$\gamma_{zzzz} \times 10^{-4}$
6-311G*	222.0	68.1
SDD[Ni]/6-31G*	221.9	55.8
ZPolX	245.3	67.7
aug-cc-pVDZ	244.7	71.9
aug-cc-pVTZ	245.2	68.0
aug-cc-pVQZ	245.4	67.6

CASSCF natural orbitals are used in the lowest-lying (ground state)  $1^1A_g$  (see Table I) the  $y_i$  parameter yields 0.17, resulting in this case in a small diradicaloid character for NiBDT. This parameter goes to 1.00 for the  $1^3B_{1u}$  state (pure diradical).

### C. Polarizabilities of NiBDT

Most of the computations for NiBDT have been performed by employing the ZPolX basis set (Table IV). In order to check its adequacy, several other sets have been employed: (i) 6-311G\*, (ii) 6-31G\*, and (iii) the series aug-cc-pVnZ, where  $n=D, T, Q$ . It is observed that ZPolX gives results in excellent agreement with the aug-cc-pVnZ series. The sets 6-311G\* and SDD[Ni]/6-31G\* give polarizability values a little smaller.

A variety of methods has been used for the computation of  $\alpha_{zz}$  (e.g., restricted and unrestricted density functional techniques, coupled cluster, and multiconfigurational perturbative methods; Table V). We would like to briefly comment on the reliability of the RCCSD/RCCSD(T) computations. The prerequisite for the reliable application of the CCSD(T) technique is that CCSD amplitudes related to the selected single determinant reference are small enough.<sup>83,84</sup> In our RCCSD calculations, one  $T_1$  amplitude was about 0.3. This is rather high and it indicates that the quasidegeneracy deteriorates the accuracy of RCCSD(T) results. However, the calculated value of  $\alpha_{zz}$ , at the RCCSD(T) level, is in reasonable agreement with that computed with the UCCSD(T) method. We consider that our most accurate value is that given by the UCCSD(T) method (Table V). Using the above value as reference we observe that: (i) correlation has a very significant effect on  $\alpha_{zz}$ , (ii) the effect of triples is much smaller in the pair RCCSD/RCCSD(T) than in UCCSD/UCCSD(T), (iii) UCCSD(T) and RCCSD(T) give values, which do not greatly differ, and (iv) there is a considerable variation in the values of  $\alpha_{zz}$  computed by the employed functionals (Table V). The present results show that dynamic correlation has a strong effect on  $\alpha_{zz}$  of NiBDT, for example,  $\alpha_{zz}[\text{UCCSD(T)}]/\alpha_{zz}[\text{UHF}] = 1.7$  (Table V).

The multiconfigurational calculations have to be checked with caution, and consider the saturation of the results with the proper enlargement of the active space. In order to check the accuracy of the active space selection, many different calibration calculations including larger number of correlating electrons (8–22) were performed. We finally concluded

TABLE V. The polarizability and second hyperpolarizability of NiBDT (the properties were computed numerically, base field of 0.005 a.u.). The ZPolX basis set was used. All values are in a.u. (conversion factors of a.u. to SI and esu are given in Ref. 85).

Method	Property	
	$\alpha_{zz}$	$\gamma_{zzzz} \times 10^{-4}$
RHF	578.0	-440.7
RCCSD	383.0	-61.9
RCCSD(T)	379.0	-307.4
UHF	211.8	6.6
PUHF	223.8	12.6
UBHandHLYP	245.3	67.7
UB3LYP	324.2	0.5
UB2-PLYP <sup>a</sup>	286.3	127.3
UCCSD	300.5	72.4
UCCSD(T)	364.3	119.0
CASSCF/CASPT2		
$m/a_1b_1b_2a_2$ <sup>b</sup>		
12/4242 ( $4\sigma 2\pi, 4\sigma^* 2\pi^*$ ) 2R <sup>c</sup>	67.9/282.2	1647.5/216.0
16/4444 ( $4\sigma 4\pi, 4\sigma^* 4\pi^*$ ) 2R <sup>c,d</sup>	243.2/340.7	1102.7/184.7
20/4646 ( $4\sigma 6\pi, 4\sigma^* 6\pi^*$ ) 2R <sup>c,d</sup>	309.3/363.8	869.5/153.1

<sup>a</sup> $\alpha_{xx} = 70.83$  a.u.,  $\alpha_{yy} = 146.99$  a.u., average polarizability  $\alpha = 168.04$  a.u.;  $\gamma_{xxxx} = 12\,597$  a.u.,  $\gamma_{yyyy} = 604\,160$  a.u.,  $\gamma_{xxyy} = 268$  a.u.,  $\gamma_{xxzz} = 6903$  a.u.,  $\gamma_{yyzz} = -59\,800$  a.u., average second hyperpolarizability  $\gamma = 356.9 \times 10^3$  a.u.

<sup>b</sup> $m$  denotes the number of active electrons;  $a_1b_1b_2a_2$  is the number of orbitals in subspaces of  $C_{2v}$  symmetry.

<sup>c</sup>Two-root state-average SA(2) CASSCF or RASSCF and corresponding multistate (MS) CASPT2 or RASPT2 level of theory. Lowest-energy root employed.

<sup>d</sup>RASSCF/RASPT2 [Ras1:  $4\sigma 2\pi$  (or  $4\pi$ ); Ras2:  $2\pi 2\pi^*$ ; Ras3:  $4\sigma^* 2\pi^*$  (or  $4\pi^*$ ), up to SDT holes in Ras1 and particles in Ras3].

that the proper extension of the active space pointed to the addition of strongly correlating  $\pi\pi^*$  MOs, that is, increasing the initial active space 12/4242 ( $4\sigma 2\pi 4\sigma^* 4\pi^*$ ) to include additional  $4\pi 4\pi^*$  or  $6\pi 6\pi^*$  MOs. These new spaces were therefore 16/4444 and 20/4646. It turns out that such spaces exceed the capability of the CASPT2 approach, therefore we had to move toward the recently developed and more flexible RASPT2 method. Three subspaces are here defined as Ras1, Ras2, and Ras3. The excitation level can be restricted in Ras1 (maximum number of holes allowed) and Ras3 (maximum number of particles), while no restriction is applied to Ras2. Following recent experience,<sup>53,86</sup> we set the excitation level to include up to three holes and three particles. In this way, the division of the subspaces for the RAS calculations 16/4444 and 20/4646 was Ras1:  $4\sigma 2\pi$  (or  $4\pi$ ), Ras2:  $2\pi 2\pi^*$ , and Ras3:  $4\sigma^* 2\pi^*$  (or  $4\pi^*$ ).

There is another source of problems that should be taken into account. As discussed in previous sections (see also Table I), two electronic singlet states are near degenerate at the employed  $D_{2h}$  geometry, in particular,  $1^1A_g$  and  $1^1B_{1u}$ . Both states will be coupled by the electric field of  $b_{1u}$  symmetry, and the addition of the field will make them to interact, and even to change order, at least in the loosely correlated levels of calculation (as CASSCF, where dynamic correlation is absent). Hence, the usual finite field perturbation theory, single state, numerical methods are not appropriate to determine NLO properties, especially because the single-state CASPT2 method yields mixed states in the lower

$C_{2v}$  symmetry group. This is therefore a two-state problem which can be solved by first running CASSCF (or RASSCF) with the average over two states and then use CASPT2 (or RASPT2) with the multistate option,<sup>56,58</sup> leading to orthogonal states, required in order to get consistently the same ground state as the lowest solution and smooth dependencies with the field for the calculation of the NLO properties. This effect is not only constrained to the MCSCF treatments but it can be more general and explain the somewhat erratic results provided by some of the methods (specifically those best behaving when applied to systems with closed-shell ground states) that are probably yielding NLO properties of higher-lying states or mixed results.

Table V incorporates results from the calculation of first polarizability of NiBDT computed at different multiconfigurational levels using three different active spaces. In all cases a two-state SA-CASSCF/MS-CASPT2 or SA-RASSCF/MS-RASPT2 procedure has been employed (SA denotes state average; MS denotes multistate). The obtained results are slightly dependent on the active space size. As compared, for instance, with the UCCSD(T) value, 364.3 a.u. (Table V), the multiconfigurational treatments require the inclusion of  $4\pi 4\pi^*$  orbital to obtain similar  $\alpha_{zz}$  values, with increasing results, when enlarging the active space. For our largest active space, the agreement (363.8 a.u.) with the UCCSD(T) value is extremely good (Table V).

## D. Second hyperpolarizabilities of NiBDT

From the results of Table V, we observe that (i) RHF, RCCSD, and RCCSD(T) fail to give even the correct sign for  $\gamma_{zzzz}$ . In fact, the RCCSD and RCCSD(T) values of  $\gamma_{zzzz}$  are considered unacceptable, for the reasons which have been explained in the previous section. (ii) UHF and PUHF give small values with the correct sign, while (iii) UB3LYP gives a very small value. The observed underestimation of  $\gamma_{zzzz}$  by UB3LYP, in comparison with the UBHandHLYP value, may be due to the percentage of the HF exchange (20% in the former, but it is 50% in the latter) and (iv) using the UCCSD(T) method as reference, the best value is given by the functional UB2-PLYP, but a reasonable value is also given by the UBHandHLYP. The UB2-PLYP functional includes 53% of HF exchange and 27 % MP2 correction.<sup>61</sup> Dynamic correlation has a great effect on the second hyperpolarizability, for example,  $\gamma_{zzzz}[\text{UCCSD(T)}]/\gamma_{zzzz}[\text{UHF}] = 18.1$  (Table V). Dynamic correlation, computed at the CASPT2 level, has a great effect on  $\gamma_{zzzz}$ . All three considered spaces give results which do not greatly differ. CASPT2, UCCSD(T), and UB2PLYP give results which are in reasonable agreement.

Similar conclusions as for the polarizability are obtained for the multiconfigurational results on  $\gamma_{zzzz}$ . In a one-state level treatment of the second hyperpolarizability CASSCF (RASSCF) yields negative values for  $\gamma_{zzzz}$  and CASPT2 (RASPT2) results several times larger than the coupled-cluster results. It is only when orthogonal solutions are provided by the two-state procedure that the results approach the UCCSD(T) value. Obviously the two-state CASSCF/RASSCF values, obtained from state-average calculations,



TABLE VI. The polarizability, second polarizability of some Ni derivatives (the B3LYP/SDD optimized geometry was employed to all calculations) (Fig. 1). All the values (a.u.) were computed by employing the UBHandHLYP/6-31G\* method. [The 6-31G\* basis set was used for C,S, and H. For Ni the SDD effective core potential (Ref. 45) has been employed.]

Molecule	$\alpha_{zz}$	$\gamma_{zzzz} \times 10^{-3}$
1	196.8	32.9
2	221.9	558
3	247.6	739
4	275.9	902
5	436.8	1535
6	805.9	7728

are not very good, but in the two-state treatment the perturbative solutions should be considered much more accurate. The results still change slightly with the active space extension. The MS-RASPT2 result for the  $\gamma_{zzzz}$  value obtained with the active space 20/4646 can be considered as the most accurate one ( $153.1 \times 10^4$  a.u.), and it is in reasonably good agreement with the UCCSD(T) value ( $119.0 \times 10^4$  a.u.). The two-state procedure, yielding orthogonal solutions for the electronic states, is required for NiBDT to obtain accurate results, when using multiconfigurational methods and numerical procedures to compute NLO properties.

### E. The effect on the properties of changes in the structure of NiBDT

Besides NiBDT, we also considered several other related Ni dithiolene derivatives. In addition we also studied TTF, in order to comment on the effect of Ni on the properties. First, we compare the properties of the pair NiBDT/TTF (Table VI). We already discussed the effect of Ni on the electronic structure (e.g., large number of low-lying excited states). This great change in the electronic structure (that is of NiBDT in comparison with that of TTF) is reflected on the  $\gamma_{zzzz}$  value of NiBDT, which is 17 times larger than that of TTF. It has been noted that a structural change, which induces many low-lying excited states, is very likely to lead to very large NLO properties.<sup>78</sup> For completeness, we note that the important consequences of using sulfur containing ligands on the electric properties has been extensively discussed.<sup>87,88</sup>

We also considered the effect of substituting one or two H atoms by CH<sub>3</sub>. Substitution of one methyl group enhances  $\gamma_{zzzz}$  by  $181 \times 10^3$  a.u., while the second CH<sub>3</sub> leads to an increase of  $163 \times 10^3$  a.u.. Remarkable is also the effect of one or two S<sub>2</sub>CS functional groups. Thus we observe (Table VI)

$$\alpha_{zz}(5) - \alpha_{zz}(2) = 215 \text{ a.u.},$$

$$\alpha_{zz}(6) - \alpha_{zz}(5) = 369 \text{ a.u.}$$

The corresponding changes in  $\gamma_{zzzz}$  are  $977 \times 10^3$  and  $6193 \times 10^3$  a.u., respectively. The observed changes in the polarizability and even more in the second hyperpolarizability are very big indeed and denote a large change in the electronic structure, which results by the above substitutions. We

observe that the larger  $\gamma_{zzzz}$  values are associated with the larger  $y_0$  values, although the largest  $\gamma_{zzzz}$  does not correspond to the largest  $y_0$  (Fig. 1).

## V. CONCLUSIONS

The polarizability ( $\alpha_{zz}$ ) and second hyperpolarizability ( $\gamma_{zzzz}$ ) of NiBDT and several of its derivatives have been computed by employing a series of basis sets and a hierarchy of methods. The ZPolX basis sets gave  $\gamma_{zzzz}$  for NiBDT in satisfactory agreement with that produced by using the series aug-cc-pVnZ, where  $n=D,T,Q$ . In order to interpret and rationalize the very large  $\gamma_{zzzz}$  value of the considered derivatives, we attempted an in depth analysis of the structure of NiBDT.

Multiconfigurational CASSCF/CASPT2 computations of the excited state structure of NiBDT show that the two low-lying singlet states, the diradicaloid  $1^1A_g$  and the ionic  $1^1B_{1u}$  state, are quasidegenerate (4 meV) at the  $D_{2h}$  planar structure. When bending the molecule the localization of the orbitals leads to true diradical structures in which the lowest singlet and triplet states become degenerate. Two significant contributions of Ni have been noted: (i) it leads to degeneracy of the  $\pi$  orbitals and (ii) it weakens the  $\sigma$  bonding structure yielding a large number of low-lying excited states. The comparison of NiBDT with TTF has shown that the latter has only one transition ( $\pi\sigma^*$ ) below 3 eV, whereas the former has 16 states in the range of the visible spectrum. In TTF, the HOMO and LUMO  $\pi$  MOs are not degenerate, unlike in NiBDT. Thus, a very large  $\gamma_{zzzz}$  value can be expected in NiBDT due to the near degeneracy and the large number of low-lying excited states. These features differentiate NiBDT from TTF, with a comparatively small  $\gamma_{zzzz}$ .

Calculation of NiBDT polarizability and second hyperpolarizability using multiconfigurational approaches help validate the UCCSD(T) obtained results. Once a large enough active space is employed and a two-level MS-CASPT2 or MS-RASPT2 procedure is used, the multiconfigurational perturbative values for  $\sigma_{zz}$  and  $\gamma_{zzzz}$ , 368.8 and  $153.1 \times 10^4$  a.u., respectively, are in close agreement with the UCCSD(T) results, 364.3 and  $119.0 \times 10^4$  a.u., respectively. The good performance of the coupled-cluster method is probably related to the fact that the singlet ground state of NiBDT does not have strictly a diradical electronic structure, but just an intermediate diradicaloid character. An essential finding of this work is the large variation of the  $\gamma_{zzzz}$  value with the structure. Specific examples are the substitution of (i) one or two hydrogen atoms by methyl groups and (ii) two or four hydrogen atoms by one or two S<sub>3</sub>C groups (Fig. 1).

*Ab initio* VB computations have given the weights of eight resonance structures. The main findings of the CASVB computations are: (i) for Ni(II) there are four diradical structures and two structures with all electrons paired and (ii) the structures with Ni(0) and Ni(IV) have negligible weight.

Three criteria for studying the DC have been considered. The functionals UBHandHLYP and UB2-PLYP give results in qualitative agreement with those computed by the CCSD(T) and CASSCF/CASPT2 methods. This is a very useful observation, because it opens the way for the system-

atic and reliable study of several much larger metal-dithiolene derivatives, which may prove to be useful for photonic applications.

## ACKNOWLEDGMENTS

We would like to thank Professor A. J. Sadlej for his generous help throughout this work. MGP would like to thank Dr G. Papavassiliou and Dr G. Anyfantis for several useful discussions. Financial support has been obtained from Project Nos. CTQ2007-61260 and CSD2007-0010 Consolider-Ingenio in Molecular Nanoscience of the Spanish MEC/FEDER.

- <sup>1</sup>R. L. Sutherland, *Handbook of Nonlinear Optics* (Marcel Dekker, New York, 1996).
- <sup>2</sup>*Non-Linear Optical Properties of Matter: From Molecules to Condensed Phases*, edited by M. G. Papadopoulos, A. J. Sadlej, and J. Leszczynski (Springer, New York, 2006).
- <sup>3</sup>H. Tanaka, Y. Okano, H. Kobayashi, W. Suzuki, and A. Kobayashi, *Science* **291**, 285 (2001).
- <sup>4</sup>S. Curelli, P. Deplano, C. Faulmann, A. Ienco, C. Mealli, M. L. Mercuri, L. Pilia, G. Pintus, A. Serpe, and E. F. Trogu, *Inorg. Chem.* **43**, 5069 (2004).
- <sup>5</sup>S. Olivier and C. Winter, *Adv. Mater. (Weinheim, Ger.)* **4**, 119 (1992).
- <sup>6</sup>J.-Y. Cho, B. Domercq, S. C. Jones, J. Yu, X. Zhang, Z. An, M. Bishop, S. Barlow, S. R. Marder, and B. Kippelen, *J. Mater. Chem.* **17**, 2642 (2007).
- <sup>7</sup>G. A. Reynolds and K. H. Drexhage, *J. Appl. Phys.* **46**, 4852 (1975).
- <sup>8</sup>J.-F. Bai, J.-L. Zuo, W.-L. Tan, J. Wei, Z. Shen, H.-K. Fun, K. Chinnakali, I. A. Razak, X.-Z. You, and C.-M. Che, *J. Mater. Chem.* **9**, 2419 (1999).
- <sup>9</sup>P. Cassoux, L. Valade, H. Kobayashi, A. Kobayashi, R. A. Clark, and A. E. Underhill, *Coord. Chem. Rev.* **110**, 115 (1991).
- <sup>10</sup>J. S. Miller and A. J. Epstein, *Angew. Chem., Int. Ed. Engl.* **33**, 385 (1994).
- <sup>11</sup>Z. S. Herman, R. F. Kirchers, G. H. Loew, U. T. Mueller-Westerhoff, A. Nazzari, and M. C. Zerner, *Inorg. Chem.* **21**, 46 (1982).
- <sup>12</sup>H. Fukui, R. Kishi, T. Minami, H. Nagai, H. Takahashi, T. Kubo, K. Kamada, K. Ohta, B. Champagne, E. Botek, and M. Nakano, *J. Phys. Chem. A* **112**, 8423 (2008).
- <sup>13</sup>C.-M. Liu, D. Q. Zhang, Y. L. Song, C. L. Zhan, Y. L. Li, and D. B. Zhu, *Eur. J. Inorg. Chem.* **2001**, 1591.
- <sup>14</sup>X. Q. Wang, Q. Ren, F. J. Zhang, W. F. Guo, X. B. Sun, J. Sun, H. L. Yang, G. H. Zhang, X. Q. Hou, and D. Xu, *Mater. Res. Bull.* **43**, 2342 (2008).
- <sup>15</sup>W. F. Guo, X. B. Sun, J. Sun, X. Q. Wang, G. H. Zhang, Q. Ren, and D. Xu, *Chem. Phys. Lett.* **435**, 65 (2007).
- <sup>16</sup>P. Aloukos, S. Couris, J. B. Koutselas, G. C. Anyfantis, and G. C. Papavassiliou, *Chem. Phys. Lett.* **428**, 109 (2006).
- <sup>17</sup>H. Yang, X. Wang, Q. Ren, G. Zhang, X. Sun, L. Feng, S. Wang, and Z. Wang, *Opt. Commun.* **256**, 256 (2005).
- <sup>18</sup>B. I. Graig and G. R. J. Williams, *Adv. Mater. Opt. Electron.* **1**, 221 (1992).
- <sup>19</sup>M. G. Papadopoulos, J. Waite, C. S. Winter, and S. N. Oliver, *Inorg. Chem.* **32**, 277 (1993).
- <sup>20</sup>C. T. Chen, S. Y. Liao, K. J. Lin, and L. L. Lai, *Adv. Mater. (Weinheim, Ger.)* **10**, 334 (1998).
- <sup>21</sup>L. Salem and C. Rowland, *Angew. Chem., Int. Ed. Engl.* **11**, 92 (1972).
- <sup>22</sup>J. Wirz, *Pure Appl. Chem.* **56**, 1289 (1984).
- <sup>23</sup>A. Sanyal, S. Chatterjee, A. Castiñeiras, B. Sarkar, P. Singh, J. Fiedler, S. Zališ, W. Kaim, and S. Goswami, *Inorg. Chem.* **46**, 8584 (2007).
- <sup>24</sup>L. Noodleman, *J. Chem. Phys.* **74**, 5737 (1981).
- <sup>25</sup>K. Ray, T. Weyhermuller, F. Neese, and K. Wieghardt, *Inorg. Chem.* **44**, 5345 (2005).
- <sup>26</sup>Y. M. Rhee and M. Head-Gordon, *J. Am. Chem. Soc.* **130**, 3878 (2008).
- <sup>27</sup>A. Thomas, K. Srinivas, C. Prabhakar, K. Bhanuprakash, and V. J. Rao, *Chem. Phys. Lett.* **454**, 36 (2008).
- <sup>28</sup>C. Prabhakar, K. Yesudas, K. Bhanuprakash, V. J. Rao, R. S. S. Kumar, and D. N. Rao, *J. Phys. Chem. C* **112**, 13272 (2008).
- <sup>29</sup>K. Srinivas, Ch. Prabhakar, C. L. Devi, K. Yesudas, K. Bhanuprakash, and V. J. Rao, *J. Phys. Chem. A* **111**, 3378 (2007).
- <sup>30</sup>V. Bachler, G. Olbrich, F. Neese, and K. Wieghardt, *Inorg. Chem.* **41**, 4179 (2002).
- <sup>31</sup>M. Nakano, H. Nagao, and K. Yamaguchi, *Phys. Rev. A* **55**, 1503 (1997).
- <sup>32</sup>M. Nakano, R. Kishi, T. Nitta, T. Kubo, K. Nakasuji, K. Kamada, K. Ohta, B. Champagne, E. Botek, and K. Yamaguchi, *J. Phys. Chem. A* **109**, 885 (2005).
- <sup>33</sup>M. Nakano, R. Kishi, N. Nakagawa, S. Ohta, H. Takahashi, S. Furukawa, K. Kamada, K. Ohta, B. Champagne, E. Botek, S. Yamada, and K. Yamaguchi, *J. Phys. Chem. A* **110**, 4238 (2006).
- <sup>34</sup>M. Nakano, R. Kishi, S. Ohta, H. Takahashi, T. Kubo, K. Kamada, K. Ohta, E. Botek, and B. Champagne, *Phys. Rev. Lett.* **99**, 033001 (2007).
- <sup>35</sup>M. Nakano, R. Kishi, S. Ohta, A. Takebe, H. Takahashi, S. Furukawa, T. Kubo, Y. Morita, K. Nakasuji, K. Yamaguchi, K. Kamada, K. Ohta, B. Champagne, and E. Botek, *J. Chem. Phys.* **125**, 074113 (2006).
- <sup>36</sup>K. Kamada, K. Ohta, T. Kubo, A. Shimizu, Y. Morita, K. Nakasuji, R. Kishi, S. Ohta, S.-i. Furukawa, H. Takahashi, and M. Nakano, *Angew. Chem., Int. Ed.* **46**, 3544 (2007).
- <sup>37</sup>K. Yesudas and K. Bhanuprakash, *J. Phys. Chem. A* **111**, 1943 (2007).
- <sup>38</sup>A. D. Buckingham, *Adv. Chem. Phys.* **12**, 107 (1967).
- <sup>39</sup>A. D. Becke, *J. Chem. Phys.* **98**, 5648 (1993).
- <sup>40</sup>C. Lauterbach and J. Fabian, *Eur. J. Inorg. Chem.* **1999**, 1995.
- <sup>41</sup>T. Kubo, A. Shimizu, M. Uruichi, K. Yakushi, M. Nakano, D. Shiomi, K. Sato, T. Takui, Y. Morita, and K. Nakasuji, *Org. Lett.* **9**, 81 (2007).
- <sup>42</sup>L. Noodleman and J. G. Norman, Jr., *J. Chem. Phys.* **70**, 4903 (1979).
- <sup>43</sup>A. Ovchinnikov and J. K. Labanowski, *Phys. Rev. A* **53**, 3946 (1996).
- <sup>44</sup>L. Serrano-Andrés, D. Klein, P. R. Schleyer, and J. M. Oliva, *J. Chem. Theory Comput.* **4**, 1338 (2008).
- <sup>45</sup><http://www.theochem.uni-stuttgart.de/pseudopotentials/clickpse.en.html>
- <sup>46</sup>J. Li and R. McWeeny, *Int. J. Quantum Chem.* **89**, 208 (2002).
- <sup>47</sup>J. Li, B. J. Duke, and R. McWeeny, VB2000, version 2.0(R3), SciNet Technologies, San Diego, CA, USA, 2009. <http://www.vb2000.net>.
- <sup>48</sup>E. D. Glendening and F. Weinhold, *J. Comput. Chem.* **19**, 593 (1998).
- <sup>49</sup>B. H. Chirgwin and C. A. Coulson, *Proc. R. Soc. London, Ser. A* **201**, 196 (1950).
- <sup>50</sup>P. O. Löwdin, *J. Mol. Struct.: THEOCHEM* **229**, 1 (1991).
- <sup>51</sup>P. C. Hiberty and G. Ohanessian, *Int. J. Quantum Chem.* **27**, 245 (1985).
- <sup>52</sup>K. Andersson, P.-Å. Malmqvist, and B. O. Roos, *J. Chem. Phys.* **96**, 1218 (1992).
- <sup>53</sup>F. Aquilante, L. De Vico, N. Ferré, G. Ghigo, P.-A. Malmqvist, T. Pedersen, M. Pitonak, M. Reiher, B. O. Roos, L. Serrano-Andrés, M. Urban, V. Veryazov, and R. Lindh, "MOLCAS 7: The Next Generation," *J. Comput. Chem.* (in press).
- <sup>54</sup>N. Douglas and N. M. Kroll, *Ann. Phys.* **82**, 89 (1974).
- <sup>55</sup>B. A. Hess, *Phys. Rev. A* **33**, 3742 (1986).
- <sup>56</sup>P.-Å. Malmqvist, B. O. Roos, and B. Schimmelpfennig, *Chem. Phys. Lett.* **357**, 230 (2002).
- <sup>57</sup>F. Jensen, *Introduction to Comp. Chem* (Wiley, New York, 1999).
- <sup>58</sup>J. Finley, P.-Å. Malmqvist, B. O. Roos, and L. Serrano-Andrés, *Chem. Phys. Lett.* **288**, 299 (1998).
- <sup>59</sup>L. Serrano-Andrés, M. Merchán, and R. Lindh, *J. Chem. Phys.* **122**, 104107 (2005).
- <sup>60</sup>C. Lee, W. Yang, and R. G. Parr, *Phys. Rev. B* **37**, 785 (1988); A. D. Becke, *J. Chem. Phys.* **98**, 1372 (1993).
- <sup>61</sup>S. Grimme, *J. Chem. Phys.* **124**, 034108 (2006).
- <sup>62</sup>A. D. Becke, *Phys. Rev. A* **38**, 3098 (1988).
- <sup>63</sup>Z. Benkova, A. J. Sadlej, R. E. Oakes, and S. E. J. Bell, *J. Comput. Chem.* **26**, 145 (2005).
- <sup>64</sup>Z. Benkova, A. J. Sadlej, R. E. Oakes, and S. E. J. Bell, *Theor. Chem. Acc.* **113**, 238 (2005).
- <sup>65</sup>A. Baranowska, M. Siedlecka, and A. J. Sadlej, *Theor. Chem. Acc.* **118**, 959 (2007).
- <sup>66</sup>T. H. Dunning, Jr., *J. Chem. Phys.* **90**, 1007 (1989).
- <sup>67</sup>R. A. Kendall, T. H. Dunning, Jr., and R. J. Harrison, *J. Chem. Phys.* **96**, 6796 (1992).
- <sup>68</sup>K. A. Peterson, D. Figgen, E. Goll, H. Stoll, and M. Dolg, *J. Chem. Phys.* **119**, 11113 (2003).
- <sup>69</sup>K. A. Peterson and C. Puzzarini, *Theor. Chem. Acc.* **114**, 283 (2005).
- <sup>70</sup>D. Figgen, G. Rauhut, M. Dolg, and H. Stoll, *Chem. Phys.* **311**, 227 (2005).
- <sup>71</sup>P. J. Davis and P. Rabinowitz, *Numerical Intergration* (Blaisdell, London, 1967), p. 166.
- <sup>72</sup>M. J. Frisch, G. W. Trucks, H. B. Schlegel *et al.*, Gaussian, Inc., Wallingford CT, 2004.
- <sup>73</sup>G. N. Schauzer and V. P. Mayweg, *J. Am. Chem. Soc.* **87**, 3585 (1965).

- <sup>74</sup>G. N. Schauzer and V. P. Mayweg, *J. Am. Chem. Soc.* **87**, 1483 (1965).
- <sup>75</sup>A. L. Bach and R. H. Holm, *J. Am. Chem. Soc.* **88**, 5201 (1966).
- <sup>76</sup>R. Benedix and H. Hennig, *Inorg. Chem. Acta* **141**, 21 (1988).
- <sup>77</sup>E. I. Stiefel, J. H. Waters, E. Billig, and H. B. Gray, *J. Am. Chem. Soc.* **87**, 3016 (1965).
- <sup>78</sup>A. Avramopoulos, L. Serrano-Andrés, J. Li, H. Reis, and M. G. Papadopoulos, *J. Chem. Phys.* **127**, 214102 (2007).
- <sup>79</sup>R. Pou-Amerigo, P. M. Viruela, R. Viruela, M. Rubio, and E. Orti, *Chem. Phys. Lett.* **352**, 491 (2002).
- <sup>80</sup>C. Adamo, V. Barone, A. Bencini, and F. Toffi, *Inorg. Chem.* **38**, 1996 (1999).
- <sup>81</sup>K. Yamaguchi, in *Self Consistent Field: Theory and Applications*, edited by R. Carbo and M. Klobukowski (Elsevier, Amsterdam, 1990), p. 727.
- <sup>82</sup>S. Yamanaka, M. Okomura, M. Nakano, and K. Yamaguchi, *J. Mol. Struct.: THEOCHEM* **310**, 205 (1994).
- <sup>83</sup>J. D. Watts, M. Urban, and R. J. Bartlett, *Theor. Chim. Acta* **90**, 341 (1995).
- <sup>84</sup>B. Jansík, V. Kellö, and M. Urban, *Int. J. Quantum Chem.* **90**, 1240 (2002).
- <sup>85</sup>M. G. Papadopoulos, J. Waite, and A. D. Buckingham, *J. Chem. Phys.* **102**, 371 (1995).
- <sup>86</sup>P.-Å. Malmqvist, K. Pierloot, A. R. M. Shahi, C. Cramer, and L. Gagliardi, *J. Chem. Phys.* **128**, 204109 (2008).
- <sup>87</sup>T. Pluta and A. J. Sadlej, *J. Chem. Phys.* **114**, 136 (2001).
- <sup>88</sup>U. Eckart, V. E. Ingamells, M. G. Papadopoulos, and A. J. Sadlej, *J. Chem. Phys.* **114**, 735 (2001).